Reactive & Functional Polymers xxx (2013) xxx–xxx

Contents lists available at SciVerse ScienceDirect

Reactive & Functional Polymers

journal homepage: www.elsevier.com/locate/react

Synthesis and structure–property relationship of polyester-urethanes and their evaluation for the regeneration of contractile tissues

Susanna Sartori [a], Monica Boffito [a,*], Piero Serafini [a], Andrea Caporale [b], Antonella Silvestri [a], Ettore Bernardi [c], Maria Paola Sassi [c], Francesca Boccafoschi [d], Gianluca Ciardelli [a,e]

[a] Politecnico di Torino, Department of Mechanical and Aerospace Engineering, Corso Duca degli Abruzzi 24, 10129 Torino, Italy
[b] Università Ca' Foscari, Department of Molecular Science and Nanosystems, Calle Larga S. Marta Dorsoduro 3246, 30123 Venezia, Italy
[c] Istituto Nazionale di Ricerca Metrologica (INRIM), Strada delle Cacce 91, 10135 Torino, Italy
[d] Università del Piemonte Orientale, Health Sciences Department, Via Solaroli 17, 28100 Novara, Italy
[e] CNR-IPCF UOS Pisa, Via Moruzzi 1, 56124 Pisa, Italy

ARTICLE INFO

Article history:
Available online xxxx

Keywords:
Polyurethanes
Mechanical properties
Peptides
Tissue engineering
Phase separation

ABSTRACT

The structure–property relationship of degradable polyurethanes from non toxic building blocks was studied by synthesising four different biodegradable poly(ester urethanes) from poly(ε-caprolactone) (PCL) diol, 1,4-diisocyanatobutane and different chain extenders. For instance, the chain extenders were an amino acid derivative diamine, an amino acid derivative diol, a cyclic diol and a custom made diamine, containing an enzymatically degradable peptide (Ala–Ala sequence). Physicochemical and morphological characterisation (SEC, DSC, DMA, AFM) was performed, showing the influence of the chain extender on the polyurethane properties. A correlation between surface domain morphologies and thermal properties was highlighted and a relationship between the biological response and surface morphologies was observed. Collecting mechanical characterisation and myoblast cell culture results together, the polyurethane synthesised with the amino acid derivative diamine resulted the most promising candidate for fabricating scaffolds supporting the regeneration of muscle tissues.

1. Introduction

The main challenge in tissue engineering is the design of biodegradable constructs with suitable properties to promote cell adhesion, proliferation and differentiation, and extracellular matrix (ECM) deposition [1]. An ideal scaffold material should mimic the surface and bulk properties of the host tissue (including wettability, elastic modulus, mechanical strength) and, additionally, include bioactive molecules (e.g. peptides) of the ECM.

Matching the mechanical properties of an artificial tissue to the graft environment is a critical point, so that progression of tissue healing is not limited by mechanical failure of the construct prior to successful tissue regeneration [2].

High molecular-weight linear aliphatic polyesters have been effectively used for clinically established products, but they possess high modulus and low elongation at break, best suited for hard tissue regeneration [3]. In order to meet the mechanical demands of force-generating contractile tissues, elastomeric polymers may serve as more appropriate raw materials for scaffold fabrication [4]. In the regeneration of muscle tissues, it should be considered that the elongation at break of the human heart was estimated to be in the range of 20–90%, with an average value of about 60% [5] and anatomical skeletal muscle exhibits strain of approximately 30–50% upon lengthening or stretching [6].

Hydrolytically degradable polyurethanes (PURs) have been used as biomaterials for several decades because of their unique physical properties and relatively good biocompatibility [7–10]. Soft degradable blocks are often comprised of degradable polyester or polycarbonate diols. Nevertheless, the degradation and remodeling of the ECM do not occur by simple ester hydrolysis, but rather by various types of proteinases [11]. To design biomimetic polymers and increase the degradation rates, enzymatically degradable PURs have been developed by introducing enzyme sensitive peptides as chain extenders [12,13].

In this work, PURs with different composition were synthesised and characterised in order to study the influence of the chain extender in their physicochemical properties and biological response. In detail, the polyurethanes were synthesised by first reacting poly(ε-caprolactone) diol (PCL) and 1,4-butanediisocyanate (BDI) to form a prepolymer; in a second step the prepolymer reacts with a chain extender to form a polyurethane. Poly(ε-caprolactone) is one of the most studied biodegradable polymer. A number of *in vitro* and *in vivo* biocompatibility and efficacy studies have been

* Corresponding author. Tel.: +39 0131 229333; fax: +39 0131 229344.
E-mail address: monica.boffito@polito.it (M. Boffito).

1381-5148/$ - see front matter © 2013 Elsevier Ltd. All rights reserved.
http://dx.doi.org/10.1016/j.reactfunctpolym.2013.01.006

performed on PCL, resulting in US Food and Drug Administration approval of several medical and drug delivery devices [14]. BDI was used as diisocyanate since the degradation product is expected to be 1,4-butanediamine (also known as putrescine), a non-toxic diamine that is, among other functions, essential for cell growth and differentiation [15]. The non toxicity of polyurethane scaffolds synthesised by PCL and BDI was partially demonstrated by Fujimoto and colleagues [16]. The authors implanted polyurethane scaffolds in the right ventricular outflow tract of adult rats: after 12 weeks the scaffolds were almost completely absorbed and just a moderate inflammatory reaction was observed.

The chain extenders used in this work were selected among easily commercially available molecules, and, in detail, were an amino acid derivative diamine (L-lysine ethyl ester), a cyclic diol (1,4-cyclohexane dimethanol) and an amino acid derivative diol (N-Boc-serinol), which can be used to funtionalise polyurethanes after deprotection of the amine group. Moreover, we synthesised a diamine containing a peptide sequence (H—Ala—Ala—NH—$(CH_2)_4$—NH_2) to tune degradability as described above. The custom made diamine was synthesised by the liquid phase method and designed in order to be enzymatically degradated in the physiological environment. This diamine contains the Ala–Ala sequence which is cleaved by elastase, a protease secreted by human neutrophils in response to inflammatory stimuli [17].

Both surface and bulk characterisations of the synthesised PURs were performed, showing the influence of the chain extender on polyurethane properties. Specifically, mechanical characterisation was performed to select the suitable materials for the regeneration of contractile tissues.

Biological tests were conducted with skeletal myoblasts (C_2C_{12} cell line) to evaluate the effect of polyurethane composition on the biocompatibility. Cell viability was studied at predefined time steps (1, 3 and 7 days) to estimate myoblast adhesion and proliferation. Cell morphology was observed at 7 days post cell seeding with a fluorescence microscope after actin and DNA staining. Western Blot analysis were conducted to evaluate the expression of both adhesion and proliferation protein markers (vinculin and proliferating cell nuclear antigen (PCNA) proteins, respectively).

2. Materials and methods

2.1. Materials

Poly(ε-caprolactone) diol (M_n = 2000 g/mol), 1,4-butanediisocyanate (BDI), dibutyltindilaurate (DBTDL) and triethylamine (TEA) were purchased from Sigma Aldrich, USA. Poly(ε-caprolactone) diol and the chain extenders were dried under reduced pressure at 40 °C overnight to remove the residual water before use. 1,4-butanediisocyanate was distilled under reduced pressure before use. In order to synthesise the peptide H—Ala—Ala—NH—$(CH_2)_4$—NH_2, putrescine (Put), di-tert-butyl dicarbonate (Boc_2O), Carbobenzoxy chloride (Cbz—Cl or Z—Cl), N,N-diisopropylethylamine (DIPEA), Palladium on carbon (Pd/C), sodium bicarbonate ($NaHCO_3$) and sodium sulfate (Na_2SO_4) were purchased from Sigma–Aldrich, Italy. L-alanine (H—Ala—OH), L-lysine ethyl ester dihydrochloride (H—Lys(H)—OEt), N-hydroxybenzotriazole (HOBt) and O-benzotriazole-N,N,N′,N′-tetramethyl-uronium-hexafluoro-phosphate (HBTU) were purchased from IRIS Bio-tech- GmbH (Germany).

All solvents were purchased from Sigma–Aldrich, Italy in the analytical grade.

2.2. Synthesis and characterisation of H—Ala—Ala—Put—H

The monoprotection of the putrescine amine group with Boc was carried out according to Zuckermann et al. procedure [18]. The diamine putrescine (Put) (11 mmol) was dissolved in 75 ml of chloroform ($CHCl_3$). Boc_2O (2.2 mmol, 1 eq. relative to the amino Put groups) dissolved in 25 ml of $CHCl_3$ was added and the mixture was stirred overnight. The solvent and the reaction byproducts were removed by low pressure distillation and the crude material was dissolved in water and filtered. The aqueous solution was extracted with dichloromethane (CH_2Cl_2). The organic layers were dried over Na_2SO_4. The yield of N-Boc monoprotected Put was 53%.

^{1}H NMR (Bruker AC200, 250 MHz, $CDCl_3$) for BocNH$(CH_2)_4NH_2$ (ppm): 3.3 (q, 2H, H_2NCH_2); 2.8 (m, 2H, BocNHCH_2); 1.6–1.4 (m; s, 13H NCH_2CH_2; Boc). Mass m/z: 188.2734.

The latter (176.0 mg, 1.0 mmol, 1 eq.) was then dissolved in 25 ml of acetonitrile (CH_3CN) and Z—Ala—OH (267.6 mg, 1.2 mmol, 1.2 eq.), HOBt (162.0 mg, 1.2 mmol, 1.2 eq.), HBTU (453.6 mg, 1.2 mmol, 1.2 eq.) and DIPEA (418.0 μl, 2.4 mmol, 2.4 eq.) were added to the solution. The reaction mixture was stirred overnight. The solvent was removed, the solid was dissolved in ethyl acetate and the organic layers were extracted with water, 5% $NaHCO_3$ and brine. The organic layers were finally dried over Na_2SO_4. The crude material was purified via flash chromatography (CH_2Cl_2/CH_3OH 95:5). The yield of Z—Ala—Put—Boc was 95%.

^{1}H NMR (Bruker AC200, 250 MHz, $CDCl_3$) for Z—Ala—NH$(CH_2)_4$NHBoc: 7.4–7.3 (5H, Z); 6.2 (mb, 1H N*H*(amide)); 5.4 (mb, 1H N*H*(Z)); 5.1 (s, 2H CH_2(Z)); 4.8 (mb, 1H N*H*(Z)); 4.2 (m, 1H Hα-Ala); 3.4–3.1 (2 m, 4H NCH_2; CH_2CH_2NHBoc); 1.6–1.4 (m; s, 13H NCH_2CH_2; Boc); 1.4–1.38 (d, 3H CH_3—Ala); Mass m/z: 393.4913.

The cleavage of the Z protecting group was carried out in methanol (MeOH) with 10% Pd/C overnight. The coupling of the second Z—Ala—OH was carried out with the same procedure and the total yield after chromatography was 80%.

^{1}H NMR (Bruker AC200, 250 MHz, $CDCl_3$) for Z—Ala—Ala—NH$(CH_2)_4$NHBoc: 7.4–7.3 (5H, Z); 6.6 (2mb, 2H N*H*(amide)); 5.3 (mb, 1H N*H*(Boc)); 5.1 (s, 2H CH_2(Z)); 4.7 (mb, 1H N*H*(Z)); 4.4 (m, 1H *H*α-Ala); 4.2 (m, 1H *H*α-Ala); 3.1 (2qb, 4H, NCH_2); 1.6–1.3 (m; 19H, NCH_2CH_2; Boc; CH_3-Ala). Finally, the Boc protecting group was cleaved in CH_2Cl_2/trifuoroacetic acid (TFA) 9:1.

^{1}H NMR (Bruker AC200, 250 MHz, D_2O) for H—Ala—Ala—NH$(CH_2)_4NH_2$ (ppm): 6.6 (2mb, 2H N*H*(amide)); 4.0 (m, 1H *H*α-Ala); 3.7 (m, 1H *H*α-Ala); 3.0 (2qb, 4H, NCH_2); 1.6–1.35 (m; s, 10H, NCH_2CH_2; CH_3—Ala). Mass m/z: 230.3123.

2.3. Synthesis of PURs

Biodegradable PURs were synthesised as previously described [19] by using poly(ε-caprolactone) (PCL) diol (M_n = 2000 Da) as soft segment in combination with 1,4-budandiisocyanate (BDI) and the following chain extenders: 1,4-cyclohexane dimethanol (CDM), L-lysine ethyl ester dihydrochloride, N-Boc-serinol or the previously described custom made peptide (H—Ala—Ala—NH—$(CH_2)_4$—NH_2). Briefly: PCL was dissolved in 1,2-dichloethane (DCE) and azeotropically dried by refluxing under nitrogen over molecular sieves for at least 8 h. The diisocyanate BDI was then added to the solution and reacted (2:1 M ratio with respect to PCL diol) with the macrodiol in the presence of the catalyst (DBTDL) to form the prepolymer. At the end of this first step (150 min, 80 °C), the chain extender was dissolved in anhydrous DCE and added at 1:1 M ratio with respect to the macrodiol at room temperature. Triethylamine was also added when L-lysine ethyl ester dihydrochloride or H—Ala—Ala—NH—$(CH_2)_4$—NH_2 were used to induce neutralisation. The chain extension reaction was stopped after 16 h by addition of MeOH. The polymer was then collected by precipitation in petroleum ether and purified by dissolution in dimethylformamide (DMF) followed by precipitation in MeOH. The obtained powder was dried under vacuum at 40 °C for 72 h.

Please cite this article in press as: S. Sartori et al., React. Funct. Polym. (2013), http://dx.doi.org/10.1016/j.reactfunctpolym.2013.01.006

2.4. PUR nomenclature

PUR nomenclature is based on the nature of the constituent segments. The first letter indicates the chain extender: C corresponds to CDM, K corresponds to L-lysine ethyl ester, NS to N-Boc-serinol and A to H—Ala—Ala—NH—$(CH_2)_4$—NH_2. The letter B corresponds to BDI, while C2000 refers to PCL with average number molecular weight M_n = 2000 Da. The nomenclature and composition of all the synthesised PURs are reported in Table 1.

2.5. Polymer characterisation

2.5.1. Infrared spectroscopy

Attenuated Total Reflectance Fourier Transform Infrared Spectra (ATR-FT-IR) of the synthesised polyurethanes were obtained at room temperature in the spectral range from 4000 to 400 cm^{-1} using a Perkin–Elmer Spectrum 100 equipped with an ATR accessory (UATR KRS5) with diamond crystal. Each spectrum, obtained as a result of 16 scans with a resolution of 4 cm^{-1}, was analysed using the Perkin–Elmer Spectrum Software. PURs samples were prepared in the form of a film using conventional solvent-casting techniques from their $CHCl_3$ or DMF solution (3%w/v).

2.5.2. Molecular weight and distribution

Number Average and Weight Average Molecular Weights (M_n and M_w), and molecular weight distribution (M_w/M_n) of the PURs were estimated by Size Exclusion Chromatography (SEC) (Agilent Technologies 1200 Series, USA). The instrument was equipped with a Refractive Index (RI) detector and two Waters Styragel columns (HT2 and HT4) conditioned at 35 °C. Tetrahydrofuran (inhibitor-free, CHROMASOLV® Plus, for HPLC, ⩾99.9%, Sigma–Aldrich, Italy) was used as mobile phase at a flow rate of 0.5 ml/min. M_n and M_w were determined by the Agilent ChemStation Software relative to the universal calibration curve. The latter was constructed based on 10 narrow polystyrene standards ranging in M_n from 740 to 18×10^4 g/mol. PURs were dissolved in tetrahydrofuran (2 mg/ml) and filtered through a 0.45 μm syringe filter (Whatman) before analysis.

2.5.3. Thermal analysis

Thermal characterisation was performed by Differential Scanning Calorimetry (DSC) using a TA Instrument DSC Q20. Each sample (weight approximately 5 mg) was encapsulated in a hermetic aluminium pan and cooled from room temperature to −60 °C by the autocool accessory of the instrument. The pan was then heated from −60 °C to 200 °C at 10 °C/min, isothermally maintained at 200 °C for 3 min, quenched to −60 °C at 20 °C/min and reheated from −60 °C to 200 °C at 10 °C/min under nitrogen atmosphere. All the thermograms were analysed using the TA Universal Analysis software. Melting temperature (T_m) was taken at the summit of the melting peak, while melting enthalpy (ΔH_m) was calculated through linear integration of the endothermic peak.

The crystallinity percentage was calculated from the first heating run in DSC experiments, through the following equation [20]:

$$C\% = (\Delta H_m \cdot 100)/(w \cdot \Delta H_m^{\circ}) \quad (1)$$

where ΔH_m is the heat of fusion of the polymer estimated as previously described, ΔH_m° is the heat of fusion of the starting 100% crystalline PCL diol (135,44 J/g [14]) and w is the PCL weight fraction in the copolymer.

Glass transition (T_g) was defined as the extrapolated onset temperature of the storage modulus change (E'), as determined by Dynamic Mechanical Thermal Analysis (DMTA) using a TA Instruments DMA Q800. Samples ($25 \times 7 \times 0.5$ mm) prepared by hot pressing were cooled at −70 °C and then uniaxially deformed in the linear viscoelastic region in tension mode at 1 Hz oscillating frequency in a nitrogen atmosphere. The samples were heated from −70 °C to 50 °C at a rate of 3 °C/min.

2.5.4. Mechanical tests

Rectangular samples ($25 \times 7 \times 0.5$ mm) of the synthesised PURs were obtained by hot pressing and mechanically characterised by stress–strain tests performed using a MTS QTest/10 Elite Controller equipped with a 500 N load cell. The cross-head speed was 10 mm/min. All PURs were tested at room temperature in dry conditions. Tensile tests were conducted in triplicate. DMTA analysis were carried out as previously described in Section 2.5.3 to characterise Storage and Loss Moduli (E' and E'', respectively), and damping coefficient ($\tan\delta$) as a function of temperature.

2.5.5. Contact angle measurements

For contact angle measurements, thin films of each PUR were prepared by spin coating (Spin CoaterLOT Oriel) a 2%w/v polymer solution in $CHCl_3$ or DMF over a rectangular glass slide (Sigma–Aldrich, Italy).

The water contact angle was measured by means of a Contact Angle Measure Instrument CAM 200 (KSV Instrument, Ltd., Finland) using a sessile drop method in advancing mode. A distilled water drop of 5 μl was gently deposited onto the surface of the sample and 5 images were recorded with a frame of 1 s and analysed using the Attension Theta software that allows an automatic curve fitting of the drop profile based on the Young and Laplace equation. In order to obtain an average result, 3 detections on different regions of the sample were acquired.

2.5.6. Atomic Force Microscopy

Intermittent-contact mode Atomic Force Microscopy (AFM) (NanoWizard II AFM, JPK Instruments, Berlin, Germany) was used to obtain phase data. Microfabricated Silicon cantilevers with force constant of about 40 N/m and fundamental frequency around 300 ± 10 kHz were used. The frequency of vibration of the cantilever was fixed near the resonance on the low-side. The ratio of the set-point amplitude to the free air amplitude of oscillation of the cantilever was maintained at 0.5. All samples were prepared by spin coating, as previously described in Section 2.5.5, in order to obtain polymer films with a thickness of about 20–40 μm.

2.6. Biological tests

2.6.1. Cell line

C_2C_{12} myoblast cells (ATCC number: CRL-1446) isolated from mouse muscle were used. Cells were cultured in Dulbecco's Modified Eagle Medium (DMEM) enriched with 10% fetal bovine serum (FBS), glutamine (2 mM), penicillin (100 U/ml) and streptomycin (100 μg/ml) (Euroclone, Italy). Cells were maintained at 37 °C in a humidified atmosphere with 5% CO_2.

2.6.2. MTS assay

MTS assay (CellTiter 96® Aqueous Non-Radioactive Cell Proliferation Assay, Promega, Italy) was performed to evaluate cell viabil-

Table 1
PUR nomenclature and composition.

PUR acronym	Macrodiol	Diisocyanate	Chain extender
K-BC2000	PCL (M_n = 2000 g/mol)	BDI	L-Lysine ethyl ester dihydrochloride
NS-BC2000	PCL (M_n = 2000 g/mol)	BDI	N-Boc-serinol
A-BC2000	PCL (M_n = 2000 g/mol)	BDI	H—Ala—Ala—Put—H
C-BC2000	PCL (M_n = 2000 g/mol)	BDI	1,4-Cyclohexane dimethanol

ity on the synthesised PURs. PUR samples were prepared in the form of a film using the conventional solvent-casting technique previously described. The obtained films (thickness of about 300 μm) were cut into squares (10 × 10 mm) and sterilized before use by washing with ethanol and exposure to ultraviolet (UV) light for 10 min each side. Cells were seeded on the positive control (cell culture Petri dish adequately treated for cell adhesion) and the different polymers at a density of 5×10^4 cells/cm^2 and cultured for 1, 3 and 7 days. At each predefined time interval, the MTS solution was added to the culture medium (100 μl each ml of culture medium). After 3 h, the solution was read in UV–VIS spectroscopy (V-630 UV–Vis Spectrophotometer, Jasco, USA) at 490 nm. The absorbance was directly proportional to viable cell amount. Experiments were conducted in triplicate.

2.6.3. Cell morphology

Cell morphology on the different substrates at 7 days of cell culture was observed with a fluorescence microscope (Leica DN2500) after actin and DNA staining with rhodamin–phalloidin and diamidino-2-phenylindole (DAPI), respectively. Images were collected by a camera connected with the microscope. Briefly, cells have been cultured on the different substrates for 7 days, fixed in PBS buffered formalin for 30 min and then labelled with phalloidin-TRITC conjugated (Sigma, Italy) which specifically binds actin filaments and DAPI (Sigma, Italy), a blue fluorescent dye specific for DNA. Cells were oserved at 40× magnification.

2.6.4. Western blots

C_2C_{12} cells were cultured for 72 h on the control and the synthesised PURs. The culture medium was then discarded and a lysis solution (SDS 2.5%, Tris–HCl pH 7.4, 0.25 M in bidistilled water) was placed on the different samples. Total proteins amount was quantified through BCA assay (Thermo Scientific, USA). For electrophoresis, 10 μg of total proteins were used. Samples were diluted with Laemmli reducing buffer (60 mM Tris–Cl pH 6.8, 2% SDS, 10% glycerol, 5% β-mercaptoethanol, 0.01% bromophenol blue) and electrophoresed on 7.5% sodium dodecylsulfate polyacrylamide gels (SDS–PAGE). The proteins were blotted onto nitrocellulose membranes. The membranes were incubated for 1 h in 5% blocking solution (non-fat dry milk in PBS), then incubated overnight with 1:500 dilution of primary antibodies (vinculin 130 kDa – Calbiochem, USA; PCNA 29 kDa – Millipore, USA; actin 42 kDa – Millipore, USA), followed by incubation with appropriate secondary antibody HRP-conjugated (Perkin-Elmer). Proteins were detected by Western Lightning plus-ECL (Perkin–Elmer, USA) and protein bands were then visualized by Bio-Rad VersaDoc™ imaging system.

2.7. Statistical analysis

Test results for mechanical properties, wettability and MTS assay are expressed as a mean ± standard deviation calculated using Microsoft Excel (Redmond, WA, USA) software. Statistical analysis was performed using SPSS version 18.0 for windows (SPSS, Inc., Chicago, IL, USA). One-way ANOVA followed by the post hoc analysis (LSD) were used to compare the results. A p value of less than 0.05 was considered as statistically significant.

3. Results and discussion

3.1. Peptide characterisation

The synthesis in solution of the dipeptide was carried out with high efficiency coupling reagents (HOBt/HBTU) giving a high purity and quantitative yields. The choice of Benzyloxycarbonil and BOC protective groups was suggested by full orthogonality and, moreover, the absence of byproducts during cleavage. The benzyl alcohol and isobutene were the only byproducts of the cleavage and were removable by low pressure distillation. The good result was confirmed by ^{1}H NMR analysis after the final cleavage.

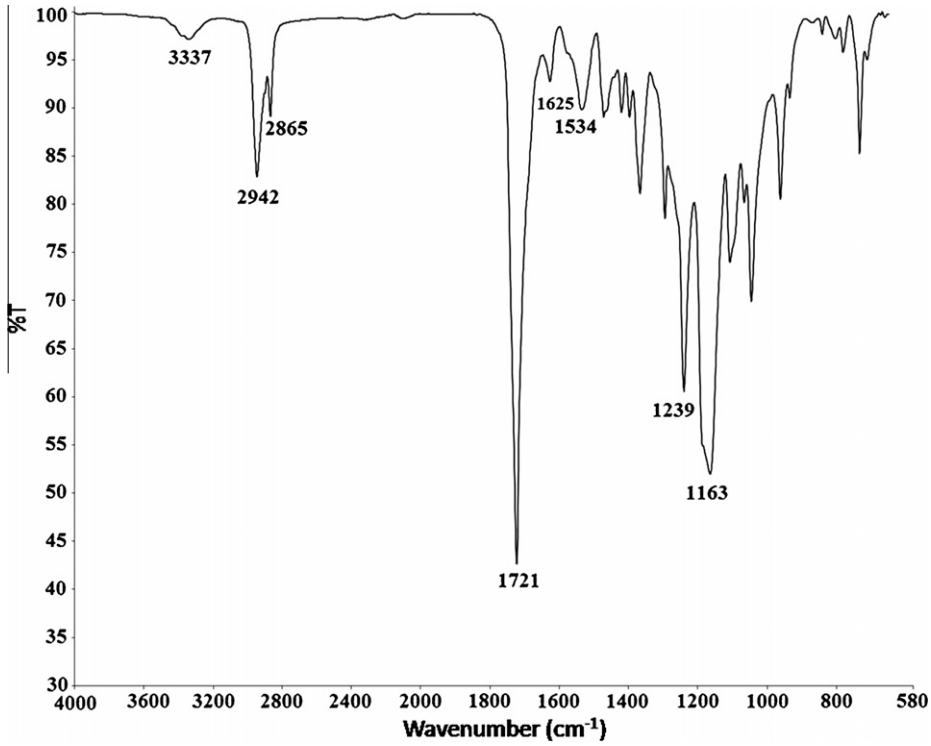

Fig. 1. ATR-IR spectrum of A-BC2000.

Table 2
Polyurethane average molecular weight data.

Sample	M_n (Da)	M_w/M_n
K-BC2000	26,000	2.0
NS-BC2000	38,000	1.6
A-BC2000	22,000	1.4
C-BC2000	15,000	1.5

Table 3
Polyurethane thermal transition data.

Sample	T_g (°C)	T_m (°C)	C (%)
K-BC2000	−50.0	25.8/42.5	22.3
NS-BC2000	−39.7	53.3	43.8
A-BC2000	−49.6	70.0	46.9
C-BC2000	−43.6	56.4	36.6

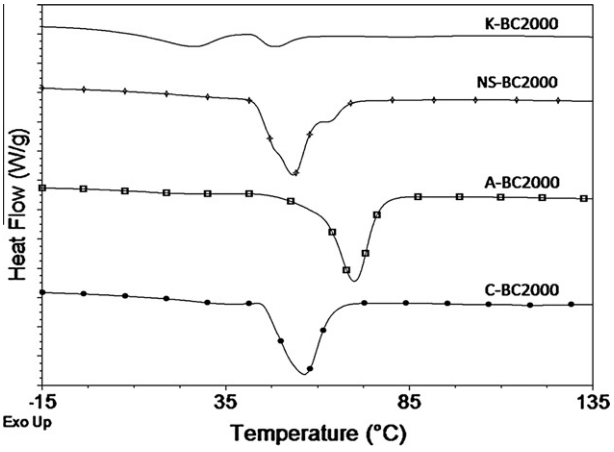

Fig. 2. DSC thermograms of the first heating cycle of the synthesised PURs.

3.2. Polyurethane characterisation

3.2.1. Chemical characterisation

All PURs were successfully synthesised as demonstrated by ATR-FT-IR spectroscopy. The four polyurethanes spectra did not show any significant difference. The spectrum of a representative polyurethane (A-BC2000) is reported in Fig. 1. The peak observable in the region between 1620 and 1640 cm^{-1} represents the stretching of C=O (amide I) and the peak at 1535 cm^{-1} represents N—H bending vibrations (amide II), indicating the formation of urethane linkages. The urethane and amide groups also showed absorption at 3340 cm^{-1} ascribed to N—H stretching. The strong absorption at 1721 cm^{-1} represents the stretching of the carboxyl group (C=O) due to ester groups in PCL.

The peak relative to N—H of the urethane group can be observed at 3337 cm^{-1} (stretching). The absorption at 1160 cm^{-1} can be ascribed to the stretching of the C—O—C linkage.

Polyurethane average molecular weights obtained by Size Exclusion Cromatography are in the range of 15,000–38,000 Da, as reported in Table 2. The low polydispersity indices of the polyurethanes indicate a narrow distribution of the molecular weights as a consequence of the good control on the polymerisation process. The quite low molecular weights obtained are not a limitation for the perspective biomedical applications of these materials, since they can improve the solubility and processability of the polymers; in the meantime, high molecular weight polyurethanes may possess high stiffness, not suitable for the regeneration of soft tissues.

3.2.2. Thermal properties

PUR thermal characterisation was performed by DSC and DMTA. Glass transition (T_g) and melting temperatures (T_m), and crystallinity percentages (C%), estimated from the melting enthalpy according to Eq. (1), are collected in Table 3. First cycle thermogram of all the analysed samples are reported in Fig. 2.

Crystallisation was attributed to the PCL segment, because the BDI-chain extender hard segments usually do not crystallise in polyurethanes with similar macrodiol-diisocyanate molar ratio [21,22]. Melting temperature varied in the range of 26–70 °C. K-BC2000 showed two melting points, relative to two different crystalline phases, and the lowest percentage of crystallinity in the polyurethane series (about 22%) which can be ascribed to the presence of pendant side segments, that prevent the polymer chains from packing closely to each other. A similar structure–crystallinity relationship cannot be observed for NS-BC2000, which possesses high crystallinity (about 44%) probably due to its higher molecular weight (M_n = 38000 Da). The higher crystallinity of A-BC2000 (approximately 47%) can be ascribed to an increase in interchain and intrachain hydrogen bonding, due to the presence of a peptide sequence in the polymer chains. However, comparative analysis should be conducted to confirm this hypothesis. The low crystallinity of C-BC2000, compared to NS-BC2000 and A-BC2000, can be partially related to its low molecular weight. However C-BC2000 showed a lower molecular weight but a higher cristallinity and melting temperature compared to K-BC2000; this behaviour can be ascribed to the cyclic structure of the chain extender, which may led to a better packing of the polymer chains leading to a more ordered crystalline structure.

Table 4
Stress strain test results.

Sample	Young's modulus (MPa)	Stress at break (MPa)	Strain at break (%)
K-BC2000	8.5 ± 0.5	9.8 ± 1.7	682.7 ± 41.3
NS-BC2000	158.7 ± 26.7	5.3 ± 0.3	141.9 ± 26.8
A-BC2000	129.2 ± 15.6	9.7 ± 2.3	22.3 ± 3.1
C-BC2000	151.8 ± 20.2	3.6 ± 0.5	3.3 ± 0.9

Glass transitions cannot be observed in the DSC recorded range; T_g values reported in Table 3 were determinated by DMTA analysis. T_g may be determined by a variety of techniques and vary in accordance with the selected method. In this work glass transitions temperatures were determined by extrapolating the onset temperature of the storage modulus (E') change, according to "E1640-09 Standard Test Method for Assignment of the Glass Transition Temperature By Dynamic Mechanical Analysis". The microphase-separated morphology of segmented polyurethanes was first suggested by Cooper and Tobolsky [23] on the basis of the glass transition temperature data from DMA analysis. In this series of PURs T_g are relative to the PCL block and in the range of −50/−40 °C, higher than that of the pure macrodiol, which is close to −60 °C [24]. These data indicate the presence of some mixing of hard segments in the soft segment phase [19]. The T_g value moves to higher temperatures with decreasing phase separation. From T_g values, K-BC2000 and A-BC2000 showed the slightly higher degree of phase separation and NS-BC2000 the lower one. However, it should be pointed out that there are small variation in T_g values (lower than 10 °C), to allow precise considerations on differences in phase separation.

3.2.3. Mechanical tests

Mechanical characterisation was performed by stress strain tests; results are reported in Table 4. Representative uniaxial stress–strain

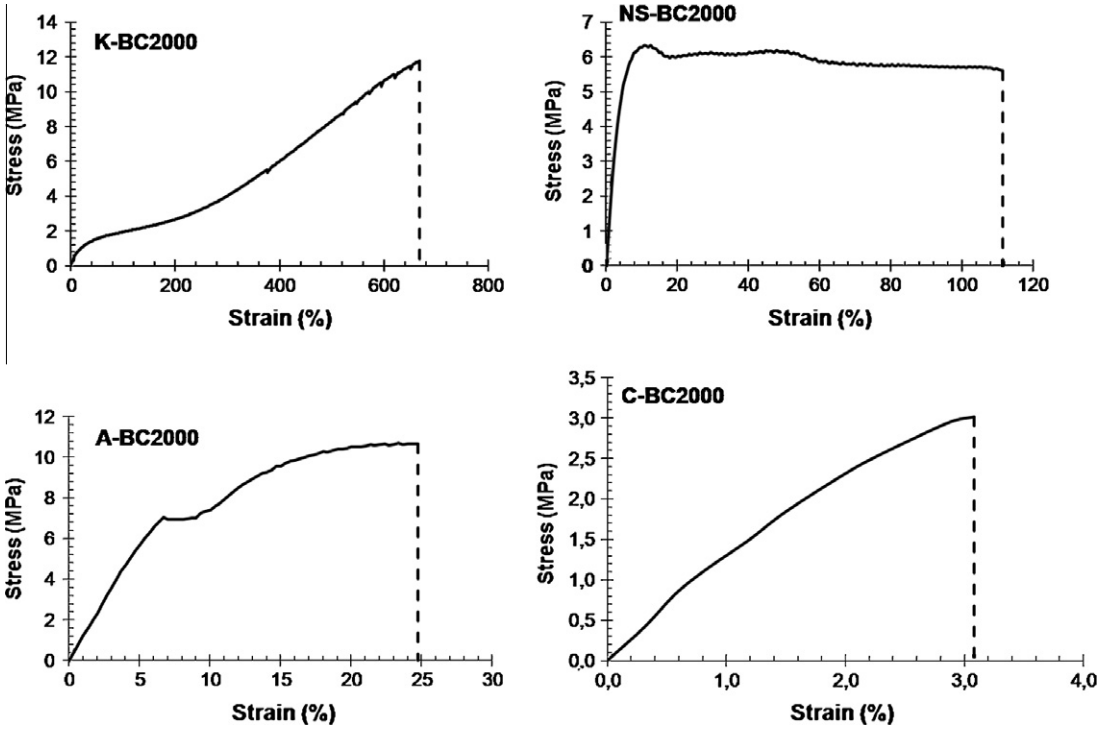

Fig. 3. Stress strain curves of the synthesised PURs.

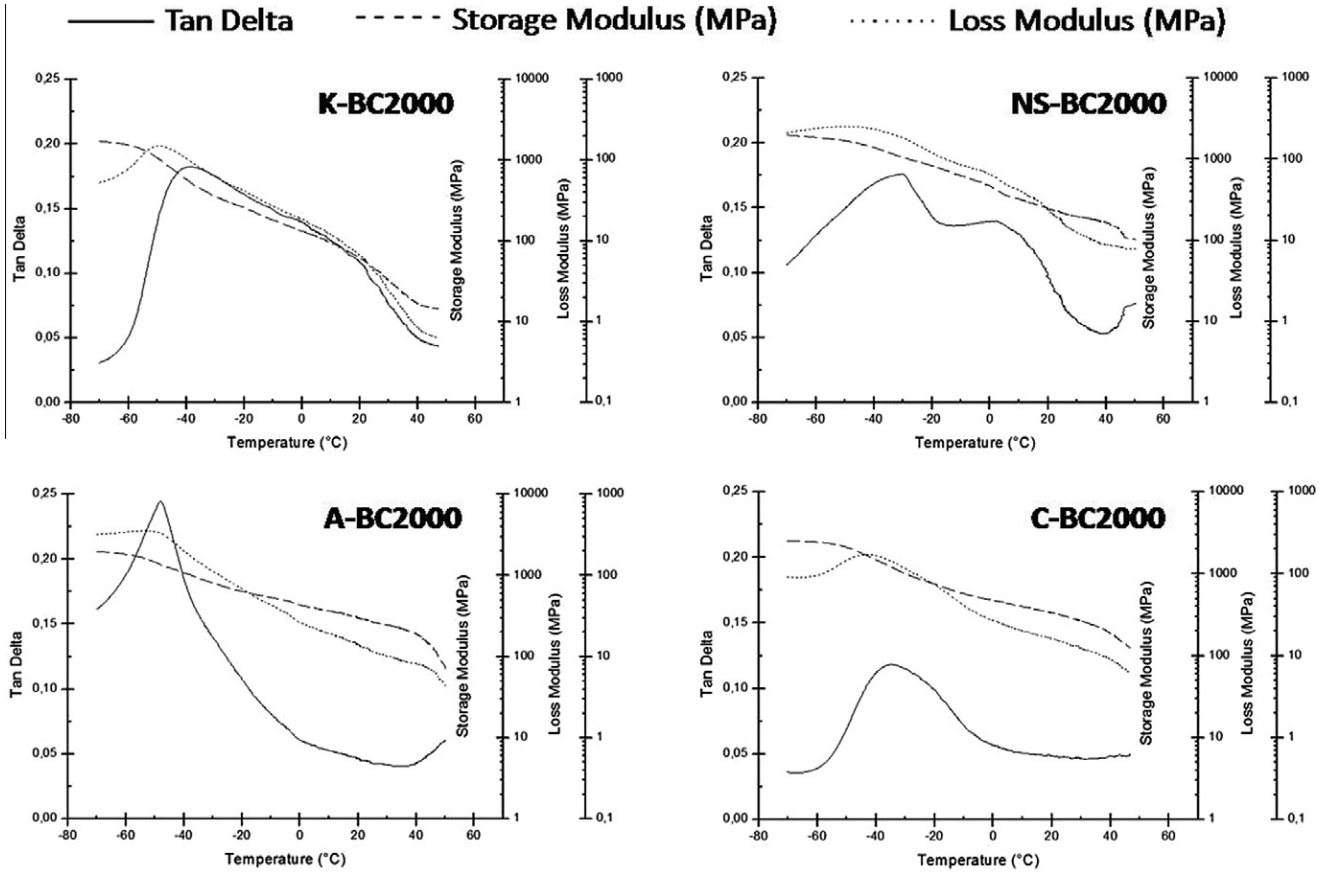

Fig. 4. DMTA analysis of the synthesised PURs.

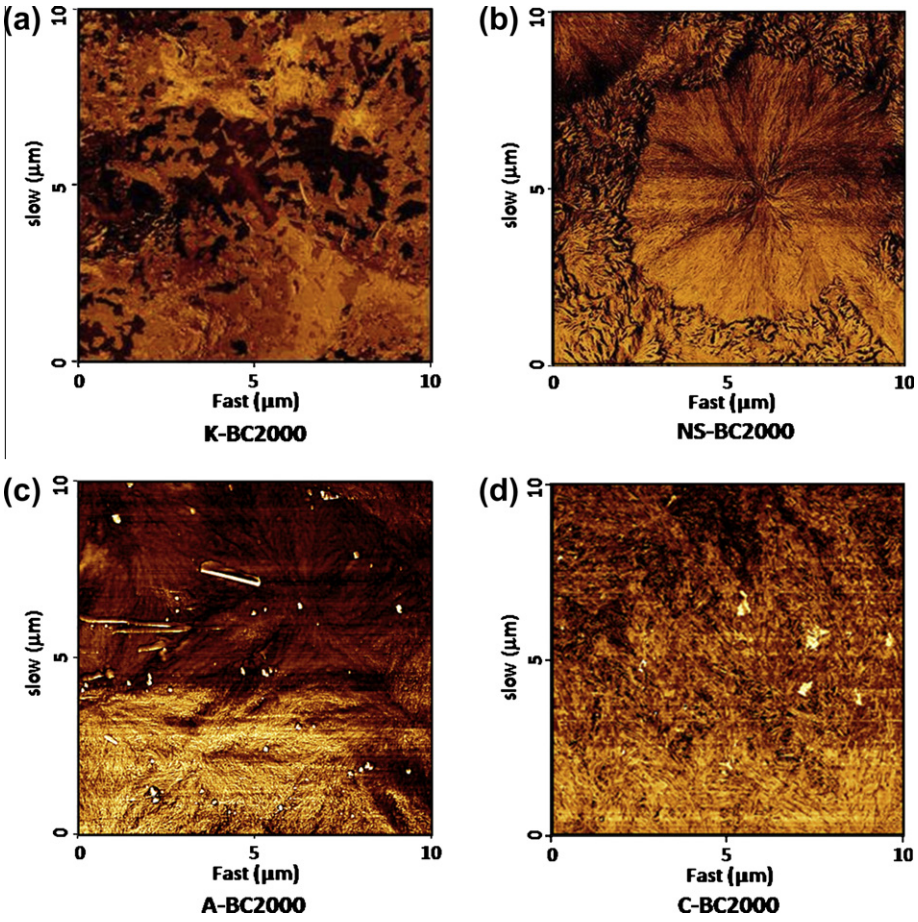

Fig. 5. High resolution AFM phase images of: (a) K-BC2000, (b) NS-BC2000; (c) A-BC2000; (d) C-BC2000.

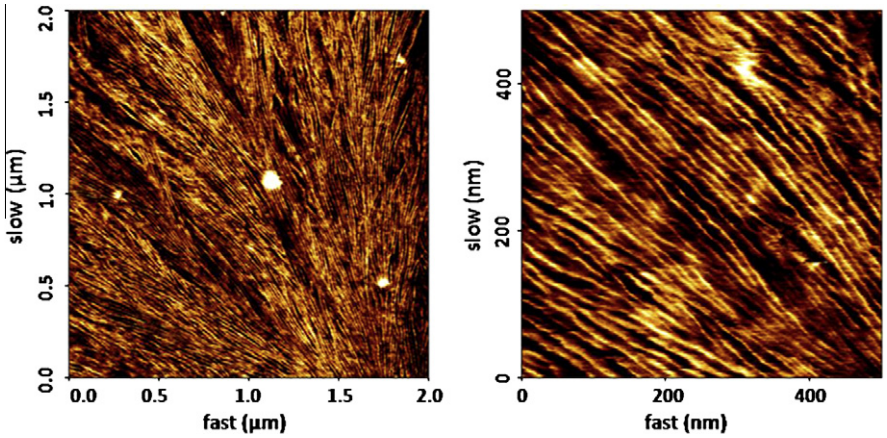

Fig. 6. High resolution AFM phase image magnifications of NS-BC2000 illustrating the fine details of microphase separated morphology.

curves of the analysed PURs are collected in Fig. 3. Young's Modulus values significantly differ ($p < 0.0001$) from one material to another, varying from 9 MPa (for K-BC2000) to roughly 159 MPa (for NS-BC2000). More in detail, K-BC2000 Young's Modulus value is significantly ($p < 0.0001$) lower with respect to that of the other synthesised polyurethanes, while no significant differences were detected between A-BC2000, NS-BC2000 and C-BC2000. Stress at break was found to be in the range of 3.6/10.3 MPa, with an upturn effect due to strain-induced crystallisation. K-BC2000 and A-BC2000 exhibited a stress at break significantly higher ($p < 0.0014$) compared to NS-BC2000 and C-BC2000.

PURs synthesised using lysine ethyl ester or N-Boc-serinol as chain extender, showed an elastomeric behaviour. Despite C-BC2000 has the lower molecular weight, it showed high Young's Modulus value and low strain at break that are in accordance with the high crystallinity and can be ascribed to the cyclic structure of its chain extender. A-BC2000 showed a slight elastomeric behaviour (strain at break is about 22%).

Although several works report that PUR mechanical properties are mainly controlled by the dominant soft segments [25], this work elucidates the influence of the chain extenders showing that they can affect both Young's Modulus value and strain at break.

Please cite this article in press as: S. Sartori et al., React. Funct. Polym. (2013), http://dx.doi.org/10.1016/j.reactfunctpolym.2013.01.006

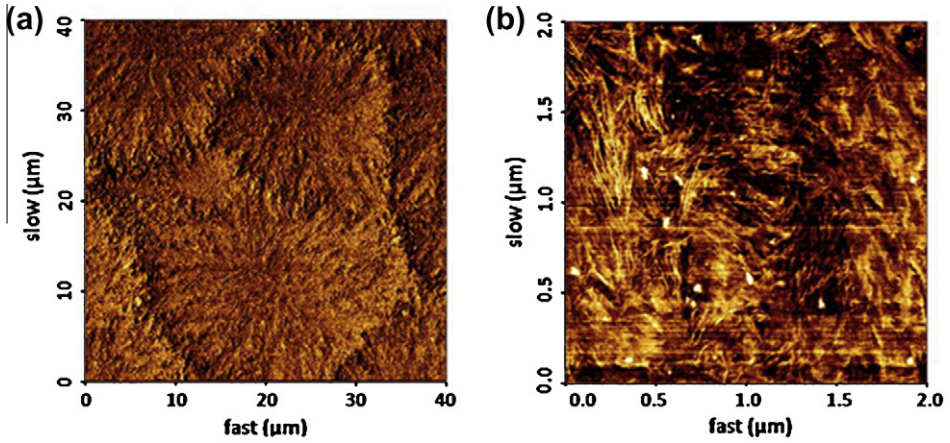

Fig. 7. High resolution AFM phase images of C-BC2000 illustrating the large spherulite morphologies (a) and the corresponding fine details (b).

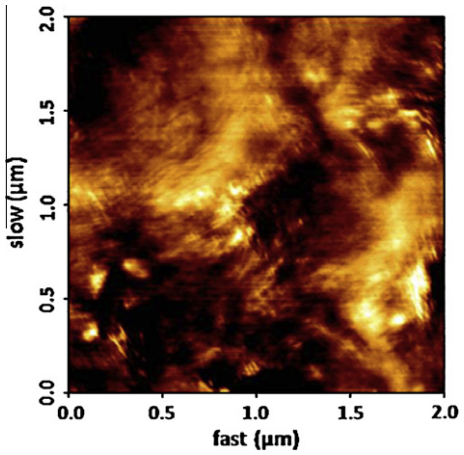

Fig. 8. High resolution AFM phase image of A-BC2000 illustrating the fine details of its microphase separated morphology.

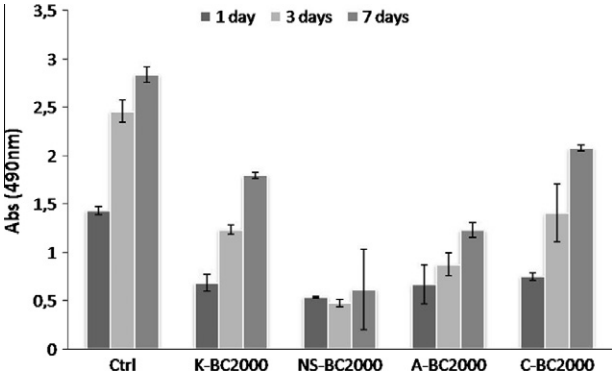

Fig. 9. Skeletal myoblast growth on polystyrene cell culture plates (positive control) and the synthesised PURs. Optical absorbance at 490 nm is directly proportional to the amount of viable cells.

Table 5
Contact angle analysis.

Sample	Contact angle (°)
K-BC2000	88.0 ± 0.4
NS-BC2000	76.1 ± 0.4
A-BC2000	88.7 ± 0.3
C-BC2000	90.6 ± 0.8

Dynamic mechanical analysis (DMA) is a useful technique for studying the viscoelastic behaviour of polymers. The temperature dependency of the storage and loss moduli of the PUR samples is shown in Fig. 4. The E' inflection in the range −60/−30 °C correlates with the peak in the loss modulus curve, E'', at the same temperatures and with the peak in loss factor, $\tan\delta$, which are attributed to T_g. A second peak in E'' can be observed at about 5 °C for NS-BC2000 and correlates with a β transition which is due to the initial mobility of the side chain segment (N-Boc-serinol). The analysis of K-BC2000 reveals a similar behaviour: Fig. 4 shows a shoulder in $\tan\delta$ which can be ascribed to a β transition, related to the mobility of the side chain segment (COOEt).

In conclusion, mechanical tests showed that K-BC2000 and NS-BC2000 are good candidates as scaffold materials for the regeneration of contractile tissues because of their elastomeric behaviour. The not marked elastomeric behaviour observed for A-BC2000 makes it unsuitable for muscle tissue regeneration, however it could be adapt as scaffold material for other soft tissues, such as tendons and ligaments [26,27].

3.2.4. Atomic Force Microscopy imaging

AFM phase imaging is a powerful tool of intermittent-contact mode AFM that provides nanometer scale information about polymer surface structures. The phase lag is very sensitive to variations in material properties such as adhesion and viscoelasticity. Phase images can provide enhanced contrast on heterogeneous surfaces, such as polymer blends and copolymers [28]. For instance, phase imaging is very useful to investigate fine features, such as lamellar structure and formation of spherulites [29].

High resolution AFM phase images of the synthesised PURs are reported in Fig. 5. Signs of the presence of hard and soft domains can be observed in all the samples, but surface morphologies appear significantly different.

With the exception of K-BC2000, spherulitic morphologies were observed. In detail, the surface of the high crystalline polyurethanes (A-BC2000 and NS-BC2000) showed banded spherulite morphologies of about 7 μm. Magnifications of AFM phase image of NS-BC2000 are reported in Fig. 6, showing the radial growth direction of the domains within the spherulite. The lamellar twisting of banded spherulites can also be observed. The thickness of the edge-on lamellae is 6.8 ± 1.7 nm as examined by AFM and analysed with ImageJ software.

Larger spherulites of about 20–30 μm can be observed for C-BC2000 in a 40 × 40 μm square image (Fig. 7a). However, the

surface of C-BC2000 resulted less homogenous and the radial growth of the domains within the spherulites is not clear resolved as in NS-BC2000 (Figs. 5 and 7b). The polymer A-BC2000 showed a lower degree of homogeneity in a 2 × 2 μm square image (Fig. 8) if compared to NS-BC2000 (Fig. 6).

3.2.5. Contact angle measurements

As shown on Table 5, all the synthesised PURs showed a moderate hydrophobic surface, with contact angle in the range of 76–90°.

Hydrophilicity is one of the thermodynamic parameters claimed to play an important role in cell adhesion. The importance of polymer surface hydrophilicity on cell adhesion was reported by Weiss [30], and confirmed by other studies. For instance, results of *in vitro* studies on the interactions of human endothelial cells with polymers, revealed that moderately hydrophilic surfaces promoted the highest levels of cell adhesion (maximum adhesion and growth at around water contact angle of 55°) [31]. However, to the best of our knowledge, any systematic study regarding the influence of hydrophobicity on myoblast adhesion, without any other synergic effect, has never been conducted. As a consequence, any undoubtedly relationship between slight variation of water contact angle and myoblast adhesion can be made.

3.2.6. Biological tests

Results of viability tests (MTS), assessed on day 1, 3 and 7 post myoblast C_2C_{12} seeding, are shown in Fig. 9.

With the exception of NS-BC2000, myoblasts C_2C_{12} cultured on the synthesised PURs showed an increase in viability from day 3 to day 7 after cell seeding indicating the ability of cells to proliferate on the materials; NS-BC2000 exhibited no significant variations in cell viability at each time step. Significant differences in cell viability from day 3 to day 7 were observed for the samples K-BC2000 ($p = 0.0008$) and C-BC2000 ($p < 0.05$). More in detail, a significant viability increase was observed for the samples K-BC2000 ($p = 0.0008$) and C-BC2000 ($p < 0.05$) at each time step analysed, while the sample A-BC2000 showed a significant increase in cell viability only from day 1 to day 7. On day 1 post cell seeding no significant differences in cell viability were observed among K-BC2000, A-BC2000, NS-BC2000 and C-BC2000. The superiority in term of cell viability of the samples K-BC2000, A-BC2000 and C-BC2000 with respect to NS-BC2000 became significant already three days post myoblast seeding. On day 7, K-BC2000 and C-BC2000 showed a significantly higher cell viability compared to A-BC2000, while no significant differences were detected between them.

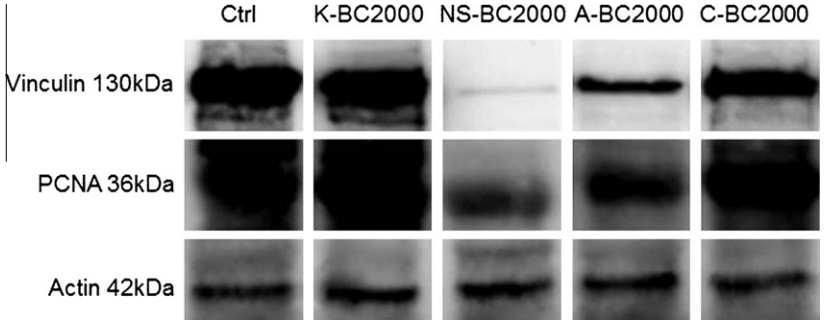

Fig. 10. Vinculin, actin and PCNA protein expression after 3 days of cell culture.

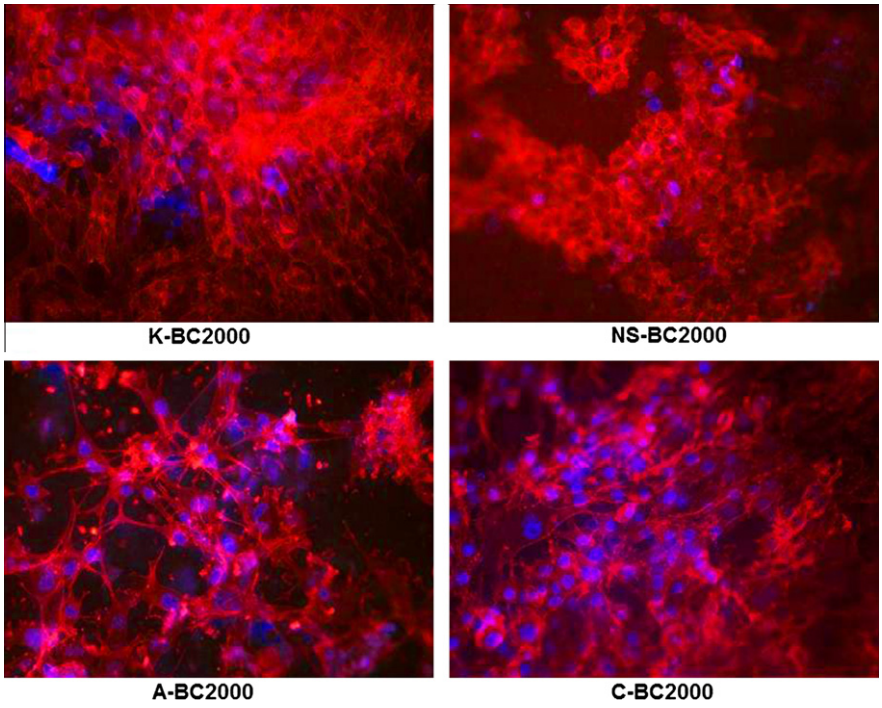

Fig. 11. Actin cytoskeleton of myoblasts cultured for 7 days on the synthesised polyurethanes. Samples were stained with phalloidin-TRITC conjugated which specifically binds actin filaments and DAPI, a blue fluorescent dye specific for DNA. (For interpretation of the references to colour in this figure legend, the reader is referred to the web version of this article.)

Please cite this article in press as: S. Sartori et al., React. Funct. Polym. (2013), http://dx.doi.org/10.1016/j.reactfunctpolym.2013.01.006

The unsuitability of NS-BC2000 was also confirmed by Western Blot (WB) analysis (Fig. 10) reporting a down-regulated expression of vinculin, a membrane-cytoskeletal protein involved in cell spreading and focal adhesion formation. On the contrary, K-BC2000 and C-BC2000 showed a vinculin expression comparable to the control, while on A-BC2000 this parameter resulted slighly down-regulated even if still indicating an appropriate cell adhesion on the substrate. Vinculin expression assessed with WB is in accordance with the results of MTS assay and morphology observations (Fig. 11). The analysis of the expression of the proliferating cell nuclear antigen (PCNA) protein at 3 days of myoblast seeding provided information about cell proliferation. The samples K-BC2000 and C-BC2000 showed PCNA protein expression approximately comparable to the positive control, while a weak decrease was observed, as expected, on NS-BC2000 and A-BC2000. The ability of cells to proliferate should be due to the synthesis of extracellular matrix proteins in the first hours of cell adhesion, promoting an adequate environment for cell proliferation.

Fluorescence staining for the f-actin component of the cytoskeleton showed in Fig. 11 illustrates how, C_2C_{12} myoblast cells have adhered and proliferated on all surfaces after 7 days. On K-BC2000, C-BC2000 and A-BC2000 substrates, actin stress fibres can be observed; cells formed a defined cytoskeletal arrangement and adopted an adequate spindle-shape morphology. NS-BC2000 does not promote myoblast spreading, since cells maintained an almost round shape. These observations confirmed the data obtained by western blot analysis on vinculin expression.

4. Conclusion

In this work the influence of the chain extender in the physicochemical properties of a series of polyester-urethanes was studied. The chemical structure of the chain extenders affects the crystallinity and the mechanical properties of the resulting polymers. In detail, crystallinity estimated by DSC analysis correlates with the morphologies of polymer thin films observed by AFM: PURs that possess the highest crystallinity (A-BC2000 and NS-BC2000) showed high order spherulitic morphologies; on the opposite, the PUR with the lowest crystallinity (K-BC2000) showed a clear phase separation but no spherulites and lamellar structures were detected.

Thermal characterisation hightlighted that all the synthesised PURs can be suitable substrates for biomedical applications. Mechanical tests showed that K-BC2000 and NS-BC2000 are good candidates as scaffold materials for the regeneration of contractile tissues because of their elastomeric behaviour.

Myoblast adhesion on the synthesised PURs was lower than that observed for the tissue culture polystyrene control; approximately 40/50% of the seeded cells adhered to the analysed substrates. Moreover, our studies on cell growth over time (3 and 7 days) demonstrated the ability of the adhered cells to spread and proliferate on the synthesised PURs, with the exception of NS-BC2000.

It is apparent from all the biocompatibility tests that C-BC2000 and K-BC2000 exhibited the best performances.

Despite some authors relate polymer biocompatibility to hydrophilicity [30,31] or to mechanical properties [32,33], we could not observe a trend in biological response related to these properties.

A relationship between phase separation and biological response was observed by Hsu [34] and Rodriguez [35]. Kohr et al. reported that heterogeneous morphologies developed by different monomer compositions of block copolymers showed different cell adhesion morphologies with regard to serum proteins [36]. Nevertheless, the detailed relationship between microphase separation and biocompatibility has not been extensively studied yet. The results reported in this work suggest a better biological response for polymers having surface with less ordered structure, as those observed in C-BC2000 and K-BC2000 by AFM studies. The poor cell adhesion of NS-BC2000 may be ascribed to its higher degree of order, compared to the other analysed polymers. However, a more detailed study should be conducted to confirm this hypothesis and comprehensive experiments concerning this aspect will be the subject of future studies.

In the series of polyurethanes studied in this work, the most promising polymer for the repair of muscle tissues was K-BC2000, since it better matched the elastomeric behaviour of muscle tissues (such as skeletal muscle and cardiac tissue) and, in the meantime, cell tests performed with myoblasts on this substrate showed high viability, adequate cell adhesion, spreading and proliferation. Additional experiments are needed to evaluate the contractile cell ability and preservation of the contractile phenotype over time.

Acknowledgment

This study was financially supported by POR Piattaforme Innovative (F.E:S.R. 2007-2013) ‘‘Active-Advanced Cardiovascular Therapies’’ and the Italian MUR PRIN2008.

Appendix A. Supplementary material

Supplementary data associated with this article can be found, in the online version, at http://dx.doi.org/10.1016/j.reactfunctpolym.2013.01.006.

References

[1] K.A. Gross, L.M. Rodríguez-Lorenzo, Biomaterials 25 (2004) 4955–4962.
[2] G.F. Muschler, C. Nakamoto, L.G. Griffith, J. Bone Joint Surg. (2004) 1541–1558.
[3] M. Sabir, X. Xu, L. Li, J. Mater. Sci. 44 (2009) 5713–5724.
[4] A.R. Webb, J. Yang, G.A. Ameer, Expert Opin. Biol. Therm. 4 (2004) 801–812.
[5] M.M. Aygen, E. Braunwald, Circulation 26 (1962) 516–524.
[6] A. Biewener, R. Baudinette, J. Exp. Biol. 198 (1995) 1829–1841.
[7] A. Silvestri, P.M. Serafini, S. Sartori, P. Ferrando, F. Boccafoschi, S. Milione, L. Conzatti, G. Ciardelli, J. Appl. Polym. Sci. 122 (2011) 3661–3671.
[8] S. Sartori, A. Rechichi, G. Vozzi, M. D'Acunto, E. Heine, P. Giusti, G. Ciardelli, React. Funct. Polym. 68 (2008) 809–821.
[9] P.A. Gunatillake, G.F. Meijs, S.J. McCarthy, R. Adhikari, N. Sherriff, J. Appl. Polym. Sci. 69 (1998) 1621–1633.
[10] G. Ciardelli, A. Rechichi, S. Sartori, M. D'Acunto, A. Caporale, E. Peggion, G. Vozzi, P. Giusti, Polym. Adv. Technol. 17 (2006) 786–789.
[11] P. Lu, K. Takai, V.M. Weaver, Z. Werb, Extracellular matrix degradation and remodeling in development and disease, Cold Spring Harb. Perspect. Biol 3 (2011) 1–2.
[12] J. Guan, W.R. Wagner, Biomacromolecules 6 (2005) 2833–2842.
[13] G. Ciardelli, A. Rechichi, P. Cerrai, M. Tricoli, N. Barbani, P. Giusti, Macromol. Symp. 218 (2004) 261–272.
[14] H. Kweon, M.K. Yoo, I.K. Park, T.H. Kim, H.C. Lee, H.-S. Lee, J.-S. Oh, T. Akaike, C.-S. Cho, Biomaterials 24 (2003) 801–808.
[15] M. Cooke, N. Leeves, C. White, Arch. Oral. Biol. 48 (2003) 323–327.
[16] K.L. Fujimoto, K. Tobita, W.D. Merryman, J. Guan, N. Momoi, D.B. Stolz, M.S. Sacks, B.B. Keller, W.R. Wagner, J. Am. Coll. Cardiol. 49 (2007) 2292–2300.
[17] N.M. Bless, D. Smith, J. Charlton, B.J. Czermak, H. Schmal, H.P. Friedl, P.A. Ward, Curr. Biol. 7 (1997) 877–880.
[18] R.N. Zuckermann, J.M. Kerr, S.B.H. Kent, W.H. Moos, J. Am. Chem. Soc. 114 (1992) 10646–10647.
[19] A. Rechichi, G. Ciardelli, M. D'Acunto, G. Vozzi, P. Giusti, J. Biomed. Mater. Res. A 84 (2008) 847–855.
[20] M. Penco, L. Sartore, F. Bignotti, S. D'Antone, L. Di Landro, Eur. Polym. J. 36 (2000) 901–908.
[21] J. Guan, M.S. Sacks, E.J. Beckman, W.R. Wagner, J. Biomed. Mater. Res. 61 (2002) 493–503.
[22] K.D. Kavlock, T.W. Pechar, J.O. Hollinger, S.A. Guelcher, A.S. Goldstein, Acta Biomater. 3 (2007) 475–484.
[23] S.L. Cooper, A.V. Tobolsky, J. Appl. Polym. Sci. 10 (1966) 1837–1844.
[24] L. Averous, L. Moro, P. Dole, C. Fringant, Polymer 41 (2000) 4157–4167.
[25] D. Sarkar, J.-C. Yang, A.S. Gupta, S.T. Lopina, J. Biomed. Mater. Res. A 90A (2009) 263–271.
[26] N. Maffulli, J. Bone Joint Surg. 81 (1999) 1019–1036.
[27] Z. Ge, F. Yang, J.C. Goh, S. Ramakrishna, E.H. Lee, J. Biomed. Mater. Res. A 77 (2006) 639–652.

[28] L. Li, C.-M. Chan, K.L. Yeung, J.-X. Li, K.-M. Ng, Y. Lei, Macromolecules 34 (2000) 316–325.
[29] B.B. Sauer, R.S. McLean, R.J. Gaymans, M. Niesten, J. Polym. Sci., Part B: Polym. Phys., 42 (2004) 1783–1792.
[30] L. Weiss, The adhesion of cells, in: G.H. Bourne, J.F. Danielli (Eds.), International Review of Cytology, Academic Press, New York, 1960, pp. 187–225.
[31] J.H. Lee, G. Khang, J.W. Lee, H.B. Lee, J. Colloid Interface Sci. 205 (1998) 323–330.
[32] T. Yeung, P.C. Georges, L.A. Flanagan, B. Marg, M. Ortiz, M. Funaki, N. Zahir, W. Ming, V. Weaver, P.A. Janmey, Cell Motil. Cytoskeleton 60 (2005) 24–34.
[33] D.E. Discher, P. Janmey, Yl Wang, Science 310 (2005) 1139–1143.
[34] S.H. Hsu, Y.C. Kao, Z.C. Lin, Macromol. Biosci. 4 (2004) 464–470.
[35] E.L. Rodriguez, R. Basar, E.G. Kolycheck, H.S. Tseng, J. Reinf. Plast. Compos. 13 (1994) 2–19.
[36] H.L. Khor, Y. Kuan, H. Kukula, K. Tamada, W. Knoll, M. Moeller, D.W. Hutmacher, Biomacromolecules 8 (2007) 1530–1540.

Please cite this article in press as: S. Sartori et al., React. Funct. Polym. (2013), http://dx.doi.org/10.1016/j.reactfunctpolym.2013.01.006